1   **System-level Insights into the Adaptation of Domestic Dairy Buffalo to Chronic**

2   **Heat Stress**

3   Zhaobing Gu [1], Shoukun Tang [2], Xianhai Fu [2], Chuanbin Liu [2], Huaming Mao*[1,2]

4

5   1 *Faculty of Animal Science and Technology, Yunnan Agricultural University, Kunming*

6   *650201, China*

7   2 *Bureau of animal husbandry and veterinary medicine, mangshi 678499, China.*

8   3 *Yunnan Provincial Key Laboratory of Animal Nutrition and Feed Science, Kunming*

9   *650201, China;*

10   *   *Corresponding authors: maohm@vip.sina.com*

11

12

13

14

Abbreviations: CATHL2 (LL-37), cathelicidin-2; CP, ceruloplasmin; GPX3, glutathione peroxidase 3; Hb, hemoglobin; HBA1, hemoglobin subunit alpha 1; HCT, hematocrit; HS, heat stress; LFQ, label-free quantification; LPL, Lipase; MCHC, mean corpuscular hemoglobin concentration; MCH, mean corpuscular hemoglobin; MCV, mean corpuscular volume; PLT, platelet hematocrit; PRM, parallel reaction monitoring; RBC, red blood cell count; ROS, reactive oxygen species; RR, Respiration rates; SRM/MRM, Single or multiple reaction monitoring; THI, Temperature-humidity index; WBC, white blood cell count; TN, thermal-neutral conditions

Abstract: Chronic heat stress (HS), aggravated by global warming, reduces the production efficiency of the buffalo dairy industry. Here, we conducted a proteomic analysis to investigate the adaptation strategies used by buffalo in response to heat stress. Seventeen differentially abundant proteins with known functions were detected using label-free quantification (LFQ), and five of these differentially expressed proteins were validated with parallel reaction monitoring (PRM). These five proteins were associated with various aspects of heat stress, including decreased heat production, increased blood oxygen delivery, and enhanced natural disease resistance. Lipase (LPL), glutathione peroxidase 3 (GPX3), cathelicidin-2 (CATHL2, LL-37), ceruloplasmin (CP), and hemoglobin subunit alpha 1 (HBA1) were shown to play cooperative roles in the tolerance of chronic HS in dairy buffalo. We found that high levels of HBA1 increased blood oxygen transport capacity. Our results increase our understanding of the adaptation of dairy buffalo to chronic heat stress.

Keywords: chronic heat stress; dairy buffaloes; proteomics; adaptation mechanisms

1. Introduction

In 2016, the global population of domestic buffalo (*Bubalus bubalis*) was ~199.0 million; about 99% of these buffalo inhabit tropical and subtropical regions [1]. At present, the mean daily maximum temperature across the regions where buffalo are raised is 19.7–41.2 ºC, but it is predicted that the daily maximum temperature in these regions will increase by 1–4.5 ºC over the next 50 years [2]. Although buffalo are well adapted to hot climates [3,4], they show signs of thermal discomfort, such as low milk yield and poor reproductive performance, at temperatures exceeding 25ºC [5]. Indeed, the body temperatures of buffalo kept at 42.1°C for 2–3 h increased from 37.5–38.5°C to 41.1°C, and the respiratory rates increased from 28.7 breaths/min to 128 breaths/min [6]. At ambient temperatures of 29.4°C and 38.9°C, nutrient intake and milk yield decreased ~30.0% and ~27.6%, respectively [7,8]. In addition, buffalo have fewer sweat glands than do cattle, increasing heat sensitivity [3,9,10]. Thus, buffalo may be increasingly prone to heat stress as global warming progresses, threatening the buffalo dairy industry [11-13].

Chronic heat stress (HS) occurs after prolonged exposure to elevated ambient temperatures and high humidity, when the animal is unable to dissipate excessive heat load to the surrounding environment [14]. HS stimulates the excessive accumulation of reactive oxygen species (ROS), which triggers the oxidative stress response [15-17]. High concentrations of ROS limit energy production and utilization in heat-stressed animals [18], negatively affecting animal growth, production, and reproductive performance [19-22]. To improve the production efficiency of dairy buffalo, it is

59   important to investigate the mechanisms underlying thermal tolerance using protein

60   biomarkers.

61   Proteomics have been widely used to assess the ability of livestock to adapt to

62   temperature increases [23]. Specifically, label-free quantification (LFQ) is a high-

63   resolution method based on mass spectrometry, which determines the relative amounts

64   of protein among two or more biological samples without the use of stable isotopes [24].

65   LFQ extracts peptide signals on the MS1 level, and thus uncouples the quantification

66   process from the identification process [25]. Single and multiple reaction monitoring

67   (SRM/MRM) methods have been widely used for protein absolute quantification due

68   to their high sensitivity, accuracy, and repeatability. Parallel reaction monitoring (PRM)

69   is high-resolution ion monitoring technique (5–6 orders of magnitude), which detects

70   all product ions in parallel in a high-precision mass spectrometer [26]. The principle of

71   this technique is similar to SRM/MRM, but PRM is more convenient and more selective

72   than SRM/MRM [27]. PRM is thus most suitable for the absolute quantification of

73   multiple proteins in a complex sample with an attomole-level of detection.

74   For livestock, blood sampling is convenient, and blood biomarkers are useful

75   indicators of the physiological state of the animal [28]. We thus hypothesized that some

76   serum proteins would be important for HS tolerance in buffalo. To address this

77   hypothesis, we aimed to detect targeted serum proteins closely related to HS with LFQ,

78   and then perform an absolute quantification of these proteins with PRM. In this way,

79   we aimed to identify candidate protein biomarkers of chronic HS to improve the thermal

80   tolerance of dairy buffalo.

2. Results

The average THI values were 75.76 and 54.26 under the HS and TN conditions, respectively ($p < 0.001$). The body temperatures of the HS and TN buffalo (38.24°C and 38.16°C, respectively) were not significantly different ($p > 0.05$). However, the RR of the HS buffalo (32.5 breaths/min) was significantly greater than that of the TN buffalo (19.0 breaths/min; $p < 0.001$).

2.1. Identification of proteins related to HS adaptation

Using LFQ, 344 low-abundance proteins were identified in the serum samples. Of these, our LFQ results indicated that 17 were differentially expressed in HS buffalo as compared to the TN buffalo (Table 1). Our volcano plot indicated that four of these proteins were more abundant in HS buffalo, while 13 were less abundant (Figure 1). Our hierarchical clustering analysis indicated that the 17 differentially abundant proteins grouped well by function: proteins similar to RETN formed one cluster, and the other cluster comprised CP (L8I5R0 and D2U6Z5), HBA1, and LL-37. L8I5R0 and D2U6Z5, both representing CP, were obviously closely clustered (Figure 2). Interestingly, four of the differentially abundant proteins identified by both LFQ and PRM were enzymes. Of these, CP (L8I5R0, D2U6Z5), HBA1 (Q9TSN7) and LL-37 (A0A0A7V3V9) were significantly more abundant in HS buffalo as compared to TN buffalo ($p < 0.05$ for all): HBA1 (3.76-fold increase), CP (1.50-fold increase) and LL-37 (1.84-fold increase) (Figure 3). The remaining enzymes, LPL and GPX3, were significantly less abundant in HS buffalo as compared to TN buffalo (0.59-fold and 0.35-fold decrease, respectively; $p < 0.05$; Table 1).

103   *2.2. GO, KEGG, and protein-protein interaction*

104   We identified three groups of GO terms that were highly enriched in the 17

105   differentially expressed proteins identified by LFQ (Table 2). One set of enriched GO

106   terms was associated with redox reactions, lipase activity, hydrolysis, and oxygen

107   transport, while a second set was associated with correct protein folding or the

108   degradation of mis-folded proteins (ubiquitin protein ligase binding, heat shock protein

109   binding, and unfolded protein binding). The third set of enriched GO terms were

110   associated with nitric-oxide synthase regulator activity (i.e., vasodilatation), ferroxidase

111   activity, and oxygen binding.

112   In parallel studies, we analyzed the correlations among the 17 differentially

113   abundant proteins identified by LFQ, and quantified the metabolites [29]. Only four

114   proteins could be mapped to KEGG metabolic pathways: GPX3, CP, CD14, and LL-37.

115   GPX3 and CP produce glutamic acid; similar amounts of glutamic acid were produced

116   by the HS buffalo (34.2 μM) and the TN buffalo (26.8 μM; $p > 0.05$). CD14 and LL-

117   37 produce acetylcholine; significantly more acetylcholine was produced by the HS

118   buffalo (0.19 nM) than the TN buffalo (0.16 nM; $p < 0.001$). GPX3 was associated with

119   the glutathione metabolism pathway; CP was associated with the porphyrin metabolism

120   pathway; CD14 was associated with the regulation of the actin cytoskeleton; and LL-

121   37 was associated with salivary secretions.

122   We analyzed the PPI networks of 16 of the 17 differentially abundant proteins

123   identified by LFQ. CD14, CPN1, HBA1, HAVCR1, CHST4, THBS4, SPARCL1 and

124   PLA1A were not included in the network (Figure 4). This network had eight edges,

125   with an average node degree of 1, and an average local clustering coefficient of 0.479.

126   The expected number of edges was 2, giving a network enrichment *p*-value of 0.000221.

127   In particular, two of the PPIs (LPL and RETN; CP and GPX3) function synergistically

128   to increase thermal tolerance in HS buffalo.

129   *2.3. Validation of LFQ results with PRM*

130   We used PRM to validate the differential abundance of five proteins: CP (L8I5R0

131   and D2U6Z5), HBA1, LPL, LL-37, and GPX3 (Table 1). Three of these proteins

132   (HBA1, CP, and LL-37) were identified as significantly more abundant in HS buffalo

133   as compared to TN buffalo by both LFQ and PRM (Figure 3). However, although LFQ

134   analysis identified GPX3 as significantly more abundant in HS buffalo, PRM did not

135   identify a significant difference in GPX3 abundance between HS and TN buffalo

136   (*p*=0.363).

137   *2.4. Biochemical blood analysis*

138   HS buffalo had significantly lower levels of MCHC ($p < 0.05$) and MCH ($p < 0.01$)

139   than did TN buffalo, and significantly higher levels of HCT ($p < 0.01$) and MCV ($p <$

140   0.01; Figure 5). Although HS buffalo had slightly higher levels of RBC, Hb, and PLT,

141   as well as slightly lower levels of WBC, these differences were not significant (Figure

142   5).

143   **3. Discussion**

144   No significant differences in body temperature were detected between the HS and

145   TN buffalo, indicating that buffalo can maintain normal body temperatures under HS

146   conditions. However, HS buffalo breathed significantly faster than TN buffalo ($p <$

147 0.001), improving respiratory evaporative heat loss. In addition to physiological

148 regulation, animals cope with high heat and high humidity primarily through

149 biochemical strategies [30]. In particular, we here identified 17 proteins that were

150 differentially abundant in HS buffalo as compared to TN buffalo. Several of these

151 proteins were associated with functions related to HS. For example, HBA1, which was

152 significantly more abundant in HS buffalo, is involved in heme and iron binding, and

153 transports oxygen from the lungs to various inner organs and peripheral tissues [31].

154 CP was significantly more abundant in HS buffalo, which plays an important role in

155 iron transport and protects cellular lipids from iron-dependent lipid peroxidation [32-

156 34]. Heat-stressed animals have poor appetites and low nutrient intake, requiring

157 efficient energy usage [35]. Under HS conditions, triglycerides are hydrolyzed by LPL

158 to free fatty acids for supplemental energy [36]. However, triglyceride degradation

159 decreases fatty acid oxidation, resulting in reduced ATP production [37]. This was

160 consistent with our results, as the HS buffalo had significantly higher LPL levels than

161 the TN buffalo.

162   Under normal condition, ROS (e.g., H_2O_2 and $O^{2\bullet-}$) play important roles as signal

163 molecules [38]. However, HS triggers excessive ROS accumulation, causing damage

164 to biological macromolecules [39]. As a well-known redox protein and antioxidant

165 enzyme, GPX3 protects cells from oxidative stress by decomposing H_2O_2 [40,41]. LFQ

166 abundance analysis indicated that HS buffalo had significantly lower levels of serum

167 GPX3 than did TN buffalo, suggesting that the HS buffalo were experiencing HS [42].

168 Consistent with this result, previous studies of livestock (e.g., finishing broilers, cattle,

169   and dairy cows) reported that HS decreased GPX3 activity. [43-46]. It is worth noting

170   that, although PRM analysis indicated that mean GPX3 levels in HS buffalo were lower

171   than those in TN buffalo, these differences were not significant. This suggested that HS

172   buffalo maintain normal GPX3 levels to protect cell membranes from oxidative damage.

173   In addition, H_2O_2 inhibits protein refolding and leads to protein denaturation, which is

174   detrimental to cellular structure and function. [47]. Indeed, several GO terms

175   significantly enriched in the differentially abundant proteins are known to promote

176   correct protein folding and degrade mis-folded proteins (i.e., ubiquitin protein ligase

177   binding, heat shock protein binding, and unfolded protein binding). This might imply

178   that buffalo use posttranslational protein processing to handle HS.

179   Chronic HS impairs immune function in animals, and also increases susceptibility

180   to infection [48]. LL-37, a small cationic antimicrobial peptide produced in the

181   epithelial cells, disrupts the activity of gram-negative bacteria by damaging and

182   destroying bacterial membranes [49,50]. LL-37 plays key roles in inflammatory

183   response regulation and immune mediator induction [51,52]. In heat-stressed mice, LL-

184   37 production was suppressed by the nicotinic acetylcholine system, increasing the

185   susceptibility of the mice *Staphylococcus aureus* [53]. In HS buffalo, LL-37 was

186   significantly more abundant than in TN buffalo (based on both LFQ and PRM),

187   suggesting that the HS buffalo might also be more susceptible to infection. As LL-37 is

188   important for the immune and inflammatory response [54,55]. it is possible that the

189   higher LL-37 serum levels seen here in HS buffalo might compensate for the relatively

190   low GPX3 levels.

191   The differential abundant proteins in HS buffalo as compared to the TN buffalo

192   were also significantly enriched in the GO term nitric-oxide synthase regulator activity,

193   which is associated with peripheral vasodilatation [56]. HS buffalo deliver more oxygen

194   per unit volume of blood than cattle [57]. In vasodilation, blood flow to the body surface

195   is increased to enhance heat dissipation, and oxygen transport to internal organs is

196   improved. This was consistent with the high levels of HBA1 and RBC detected in the

197   HS buffalo.

198   We were unable to identify metabolic (KEGG) pathways enriched in most of the

199   17 differentially abundant proteins identified by LFQ. However, we successfully

200   mapped four proteins (GPX3, CP, CD14 and LL-37) and their corresponding

201   metabolites to metabolic pathways. As a major neurotransmitter in animals,

202   acetylcholine participates in homoeothermic thermoregulation [58]. Acetylcholine is

203   also known to regulate glutamic acid release, and glutamic acid generates glutamate via

204   pyroglutamic acid [59]. Glutamate and GPX produce glutathione via the glutathione

205   metabolism pathway [60], and GPX3 and glutathione protect the cell from heat injury

206   [61]. Glutamic acid, along with CP, is also involved in the porphyrin metabolism

207   pathway, which increases HBA1 levels to improve oxygen transport in HS animals. LL-

208   37 and acetylcholine were mapped to the salivary secretion pathway. As buffalo, which

209   have few sweat glands [3], dissipate only 12% of their excess heat through skin

210   evaporation [9]; salivary secretions have been shown to help decrease body temperature

211   [62,63].

212   Under HS conditions, high levels of hemoglobin lead to increased oxygen delivery

213   [64]. Based on these pathways and our results, we propose a model of HS adaptation in

214   dairy buffalo (Figure 6): an increase in HBA1 abundance to eliminate ROS and

215   maintain normal oxygen supply, and an increase in LL-37 abundance to enhance host

216   disease resistance. PPI networks provide collaborative working modes for

217   physiological and biological processes at the system-level [65]. We found that most of

218   the 17 differentially abundant proteins in HS buffalo as compared to TN buffalo were

219   linked in the *H. sapiens* database (Fig. 4). CD14, CHST4, HBA1, SPARCL1, CPN1,

220   THBS4, SPARCL1, and PLA1A were not linked to each other, possible because these

221   proteins have dissimilar functions.

222   It is well known that Hb and CP play a collaborative role in oxygen delivery, as

223   CP oxidizes $Fe2+$ to $Fe3+$ without releasing ROS [66]. Indeed, we observed a

224   concomitant increase in Hb and CP in HS buffalo, consistent with a previous study [54].

225   However, to date, no biological interaction networks have shown a direct relationship

226   between these proteins, although CP was shown to have an inverse linear relationship

227   with soluble transferrin receptor levels [67]. Therefore, we speculated that Hb might

228   have an indirect relationship with CP. That is, these proteins were not linked in the PPI

229   network, but Hb and CP are functionally similar, and their serum levels increased

230   simultaneously. Previous studies have reported that RETN and LPL are important for

231   glucose and lipoprotein metabolism [68], and the PPI between RETN and LPL

232   indicated that the metabolic profiles of glucose and lipoprotein were altered by HS.

233   Moreover, the enzymatic oxidant GPX3 and the nonenzymatic antioxidant CP protect

234   the cell from damage due to oxidative stress [69].

235   YWHAZ (P63103), YWHAE (P62261; 14-3-3E), and YWHAG (A7Z057) are

236   isoforms of 14-3-3 proteins, which act as molecular chaperones [70]. YWHAZ

237   negatively regulates cell death, and YWHAE facilitates the movement of

238   phosphorylated HSF1 from the nucleus to the cytoplasm, increasing cell

239   thermotolerance. The three 14-3-3 proteins were downregulated in the HS buffalo,

240   suggesting that other proteins may perform these biological functions under HS.

241   Under HS, homoeothermic animals facilitate heat dissipation by increasing body

242   temperature, respiratory rate, and blood flow to the peripheral tissues [71,72]. The

243   demands on the cardiovascular system also increase with HS, as does arterial blood

244   pressure, causing internal tissues and organs to compete with peripheral areas for blood

245   supply [73,74]. Eventually, low blood flow volume may result in the hypoxia of the

246   internal organs [75]. Indeed, body temperature and blood flow may be closely

247   associated [76]: it was shown that blood flow to internal organs, such as the

248   reproductive organs, decreased 20–40% in heat-stressed rabbits [77].

249   During HS, RBC decrease [78]. Indeed, HS cattle decreased ~12–20% as

250   compared to TN cattle [79]. Here, the RBC of the HS buffalo was not significantly

251   different from that of the TN buffalo. This might indicate HS buffalo protect RBCs from

252   heat injury. Hb is associated with the delivery of oxygen from the lungs to various other

253   tissues [80]. An increase in serum Hb may compensate for a decrease in RBC and low

254   MCV, enabling the maintenance of normal oxygen supply under chronic HS. It may be

255   that high levels of serum Hb protect the red blood cells from oxidative stress [81,82].

256   Hb increases have been reported in several other animal species subjected to HS,

257   including sheep, goats, piglets, ruminants (Holsteins, Jerseys, and Zebus), and tilapia

258   [83-88].

259   Hb increases may be due to low oxygen pressure and saturation, or to an improved

260   resistance to ROS [89]. In contrast, cooling increased blood Hb concentrations in HS

261   Murrah buffalo [90]. Thus, high Hb levels may alleviate the deleterious effect of HS

262   and hypoxia. However, one study showed that HS decreased blood Hb concentration as

263   compared to normal temperatures [91]. which may be because the acute HS animals in

264   that study were exposed to extremely high temperatures ($40 \pm 2°C$). Here, the chronic

265   HS buffalo had higher serum Hb as compared to TN buffalo. The HS buffalo also had

266   significantly higher concentrations of HBA1 than the TN buffalo, indicating that high

267   HBA1 concentrations may alleviate the tissue and organ hypoxia caused by an

268   increased respiratory rate. Indeed, it has been shown that HBA1 plays an important role

269   in increasing blood flow to peripheral tissues. HS buffalo also had significantly lower

270   levels of MCHC and MCH, as well as significantly higher levels of HCT and MCV.

271   This might indicate that dairy buffalo under chronic HS maintain a normal oxygen

272   supply by modulating crucial blood parameters.

273   HS animals decrease nutrient intake, leading to a negative energy balance7.

274   Because fatty acid oxidation produces more heat (146 ATP) than does carbohydrate (38

275   ATP), heat-stressed animals decrease fatty acid oxidation [7,92]. LPL is synthesized at

276   the surface of the vascular endothelium and released into the blood. LPL hydrolyzes

277   circulating triacylglycerides to free fatty acids, promoting fat synthesis while

278   decreasing the production of ATP and heat [93]. In addition to decreasing heat

279   production, fat deposition is beneficial under HS as fat insulates the body to decrease

280   solar radiant heat absorption [94]. Indeed, low levels of glycerol in the plasma of

281   ruminants were found in summer [95]. However, few studies have focused on serum

282   profiles of LPL abundance. LPL levels in pig adipose tissue increased in response to

283   mild HS [96]. as did adipogenesis in porcine adipocytes [97]. LPL activity increased in

284   the plasma and muscle of HS rats, but not in the white adipose tissue [98]. We found

285   that serum LPL abundance decreased in response to chronic HS. We thus speculated

286   that dairy buffalo, unlike monogastric animals, adapt to chronic HS by decreasing fatty

287   acid oxidation to reduce heat production. Based on the HS-related functions of LL-37

288   (physiological defense response), ceruloplasmin (copper ion binding and ferroxidase

289   activity), and HBA1 (oxygen delivery), as well as the associated metabolites, we

290   proposed a model of the anti-HS adaptive mechanisms used by dairy buffalo to cope

291   with chronic HS (Figure 6).

292   **4. Materials and Methods**

293   *4.1. Animals*

294   Animals were treated according to the strictures of the Animal Welfare Act, as

295   issued by Animal Ethics Committee of Yunnan Province, China in 2007. All animals

296   were loose housed, and provided with fresh drinking water ad libitum. Animals were

297   fed mixed rations (80% whole-plant corn silage ad libitum, 12.5% feed concentrate,

298   and 7.5% corn protein powder).

299   The temperature-humidity index (THI) was calculated based on air temperature

300   and relative humidity. As THI is closely related to the body temperatures of dairy

301   animals under HS, THI is widely used to assess the degree of HS [99]. THI values ≥72

302   have been shown to affect dairy cattle [100]. In Dehong, Yunnan province, China

303   (24.43ºN, 98.57ºE; altitude: 870 m), average THI has been ≥72 between June and

304   August 2005–2015, based on meteorological data. Therefore, six multiparous Nili-Ravi

305   × Murrah × local crossbred female buffaloes (group HS; daily average milk yield 4.5

306   kg) with similar lactation were used for the heat stress experiment at this site between

307   July 20 and August 4, 2016 (average THI 75.76). We tested another six dairy buffaloes

308   (daily average milk yield 6.1 kg) under thermal-neutral conditions (group TN) between

309   January 3 and January 18, 2017 (average THI 54.26).

310   *4.2. Environmental and physiological parameters*

311   Temperature and humidity loggers (±0.2°C; Testo 175H1), placed 2.0 m above the

312   floor of the bedding area, recorded ambient temperature and relative humidity at 30 min

313   intervals. We used these figures to calculate THI: $THI = (1.8 \times T + 32) - (0.55 - 0.0055$

314   $\times RH) \times (1.8 \times T - 26)$ [89], where T was the ambient temperature (°C) and RH was

315   the relative humidity (%).

316   Respiration rates (RR; breaths/min) were measured daily at 08:00, 13:00, and

317   18:00 h using a stopwatch. A waterproof micro-temperature sensor (±0.5°C; DS1922L,

318   Wdsen Electronic Technology Co., Ltd), fixed in the slot of a T-shaped controlled

319   internal drug release device (without progesterone; DEC International NZ Ltd), was

320   placed in the vagina of each buffalo. This device recorded body temperature at 30 min

321   intervals.

322   *4.3. Depletion of high-abundance proteins from the serum*

323   Blood samples were collected with vacutainer tubes via jugular venipuncture.

324   Each sample was centrifuged at 1400 g for 10 min to separate the serum. Serum samples

325   were stored at -80°C. High-abundance proteins in the serum samples were depleted

326   using affinity chromatographic columns (Agilent Multiple Affinity Removal LC

327   Columns). The low-abundance proteins in the serum samples were isolated by first

328   performing an ultrafiltration concentration, then adding one double volume of SDT

329   buffer (4% SDS, 100 mM Tris-HCl, and 1 mM DTT; pH 7.6) to the concentrated sample.

330   The resultant mixture was then incubated in a boiling water bath for 15 min. The

331   mixture was then centrifuged at 14000 g for 20 min, and the supernatant was removed.

332   We then added 20 µg of the supernatant to 5×loading buffer (10% SDS, 0.5%

333   bromophenol blue, 50% glycerol, 500 mM DTT, and 250 mM TrisHCl; pH 6.8). This

334   mixture was incubated in a 90°C water bath for 5 min, and then analyzed using 12.5%

335   SDS-PAGE (constant 14 mA current for 90 min) with Coomassie blue staining.

336   *4.4. Filter-added sample preparation protein digestion*

337   Trypsin protein digestion was performed using the filter-aided sample preparation

338   (FASP) procedure described previously [101]. In brief, serum samples were lysed, and

339   proteins were extracted using SDT buffer. Proteins were quantified with BCA Protein

340   Assay Kits (Bio-Rad). We then analyzed 20 µg of each extracted protein sample with

341   SDS-PAGE. Next, 100 µg of extracted protein was dissolved in DTT (to generate a

342   final concentration of 10 mM) in a 90°C water bath for 15 min, and then cooled to room

343   temperature. Small molecules and detergent were extracted using 10 kD ultrafiltration

344   with 200 µL UA buffer (8 M Urea and 150 mM Tris-HCl; pH 8.0). The mixture was

345 centrifuged four times at 14,000 g for 30 min, and the filtrate was discarded. We then

346 added 100 IAA buffer (50 mM IAA in UA buffer) to the concentrate. Prior to

347 centrifugation, this mixture was shaken at 600 rpm for 1 min, and then incubated for 30

348 min in the dark. After incubation, the mixture was centrifuged at 14000 g for 20 min.

349 The filter was washed three times with 100 µL of UA buffer and centrifuged at 14000

350 g for 20 min. Then, the filter was washed twice with 100 µL of 50 mM NH4HCO3

351 buffer. Finally, the protein suspension was added to 40 µL of NH4HCO3 buffer (2 µg

352 Lys-C) and incubated in a 37°C water bath for 4 h. We added 2 µg trypsin to the protein

353 mixture, and then incubated the mixture in a 37°C water bath for 16 h. After incubation,

354 the protein mixture was transferred to a fresh reaction tube, and centrifuged at 14000 g

355 for 15 min. Finally, the filter was washed with 40 µL of 50 mM NH4HCO3 buffer, and

356 centrifuged at 14000 g for 30 min. The filtrate was collected and desalinated with a C18

357 Cartridge (Empore SPE Cartridges C18 [standard density], Sigma; bed inner diameter

358 7 mm; volume 3 ml). Desalted samples were freeze-dried, and peptide levels were

359 determined at OD280. Peptide samples were then stored at −80°C.

360 *4.5. LFQ with LC-MS/MS analysis*

361   We performed relative LFQ with LC-MS/MS. LC-MS/MS was performed using a

362 Q-Ex active mass spectrometer (Thermo Scientific) coupled to an Easy nLC 1200

363 (Proxeon Biosystems, now Thermo Fisher Scientific) with an analysis time of 60 min.

364 First, peptides were loaded onto a reverse phase trap column (Thermo Scientific

365 Acclaim PepMap100; 100 µm × 2 cm; nanoViper C18) connected to a C18-reversed

366 phase analytical column (Thermo Scientific Easy Column; 10 cm long, 75 µm inner

367   diameter, 3 μm resin) in buffer A (0.1% formic acid). Peptides were separated using a

368   linear gradient of buffer B (84% acetonitrile and 0.1% formic acid) at a flow rate of 300

369   nl/min, controlled by an IntelliFlow technology. The linear gradient in the trap column

370   was as follows: 0–35% solution B from 0–50min; 35–100% solution B from 50–55min;

371   40–100% solution B from 55–60min; and hold at 100% solution B.

372   MS raw data for all samples were combined and searched using MaxQuant

373   v1.3.0.5 [102], which uses the Andromeda search engine against the Bovinae Uniprot

374   database [103]. The precursor mass tolerance was set to 20 ppm for the first Andromeda

375   search, and to 6 ppm for the main search. Carbamidomethylation (C) was considered a

376   fixed modification, while oxidation (M) and acetylation (of the protein N-terminus)

377   were considered variable modifications. We eliminated all peptide and protein

378   identifications where the false discovery rate (FDR) was >0.01 against the reversed-

379   sequence database.

380   We used the MaxLFQ approach in MaxQuant for label-free quantification [104],

381   enabling 'match between runs' with a retention time window of 2 min, and setting the

382   LFQ minimum ratio count to 1. Using the relative abundance of proteins in TN buffalo

383   as a reference, we identified HS-buffalo proteins as significantly differentially

384   expressed if the HS protein was identified in at least two of three replicates with a fold

385   change >1.5 and a p <0.05. We used volcano plots to visualize the differentially

386   expressed proteins. We then performed a hierarchical clustering analysis of the proteins

387   differentially expressed between the HS and TN buffalo using the log2-transformed

388   expression values and a cutoff of $p < 0.05$ in Treeview (Java Runtime Environment)

389   [105].

4.6. Absolute quantification of targeted proteins with PRM

391   The Easy nLC 1200 (Thermo Scientific) was used for chromatographic separation.

392   First, peptides were separated with a binary solvent system consisting of 0.1% formic

393   acid (solvent A) and 0.1% formic acid acetonitrile (84% acetonitrile) (solvent B). We

394   used 95% solvent A as the equilibrium liquid for the analytical column

395   (ThermoScientific EASY column). We added 20 fmol of a standard peptide to 2 µg of

396   the separated peptides. The peptide mixture was then separated at a flow rate of 250

397   nl/min, with a linear gradient in the trap column (5–23% solution B from 0–42 min;

398   23–40% solution B from 42–50 min; 40–100% solution B from 50–60 min; and hold at

399   100% solution B).

400   We only selected proteins for PRM validation that were significantly more

401   abundant and closely associated with heat stress adaptation. We examined the peptides

402   eluted by the nano-high-performance LC using PRM positive ion mass spectrometry

403   on a Q-Ex active HF mass spectrometer system (Thermo Scientific). MS spectra were

404   acquired in the m/z range 300–1800, with an R of 60000 at m/z 200. Automatic gain

405   control (AGC) was set to 3e6, with a max injection time of 200 ms. We then selected

406   20 PRM/MS2 scans for higher-energy collisional dissociation experiments that

407   conformed to the following parameters: 1.6 Th isolation window; R of 30,000 at m/z

408   200; 3e6 AGC; 120 ms maximum injection time; MS2 higher-energy collisionally

409   activated dissociation (HCD); and a normalized collision energy of 27.

410   We analyzed the PRM raw data from the 12 HS and TN samples with Skyline

411   v3.5.0 [106]. The peptide settings used for the Skyline import were consistent with the

412   MaxQuant search parameters (i.e., enzyme set to trypsin; max missed cleavages set to

413   2). For each set of Skyline analyses, we selected two or three consecutive high-intensity

414   peptides for import into Skyline. Skyline was used to determine the number of targeted

415   proteins, the sequences of the targeted peptides, the charges of the parent ions, and the

416   peak areas. Total peak areas were calibrated against internal standard peptides, heavy

417   isotopes (absolute quantification) [94]. Based on these total peak areas, we quantified

418   each target peptide.

419   *4.7. Bioinformatics analysis*

420   We identified protein sequences homologous to those of the selected differentially

421   expressed proteins with the NCBI BLAST+ client (ncbi-blast-2.2.28+-win32.exe) and

422   InterProScan [107,108]. We then annotated protein sequences using gene ontology (GO)

423   terms with Blast2GO [109,110]. The GO annotation results were plotted with R scripts.

424   Following annotation, the differentially expressed protein sequences were blasted

425   against the Kyoto Encyclopedia of Genes and Genomes (KEGG) database

426   (http://geneontology.org/) to identify KEGG orthology. Differentially expressed

427   proteins were subsequently mapped to KEGG pathways [111].

428   Finally, we constructed a functional protein interaction network for our

429   differentially expressed proteins using STRING (https://string-db.org/), searching by

430   multiple protein names. As few protein–protein interactions (PPI) are yet available in

431   the *Bos taurus* database of STRING, we searched for these interactions in the *Homo*

432   *sapiens* database instead.

433   *4.8. Biochemical parameters*

434   We measured hemoglobin level (Hb), red blood cell count (RBC), white blood cell

435   count (WBC), hematocrit (HCT), mean corpuscular hemoglobin concentration

436   (MCHC), mean corpuscular hemoglobin (MCH), platelet hematocrit (PLT), and mean

437   corpuscular volume (MCV) in the whole blood samples using a fully automated

438   biochemical analyzer (Sysmex XT-1800i) within 24 h of blood collection.

439   **5. Conclusions**

440   Our results indicated that, in buffalo, pathways associated with oxidation-

441   reduction, hydrolysis, protein-mis-folding repair, and oxygen transport were activated

442   by chronic HS, and that LPL, GPX3, LL-37, CP, and HBA1 played cooperative roles

443   to mitigate the effects of chronic HS. Our results, along with our newly developed

444   model, increase our understanding of the adaptation to heat stress in dairy buffalo. Our

445   results will thus help to support the vigorous development of the buffalo dairy industry

446   in tropical and subtropical regions.

453

454   **Figure 1.** Quantitative proteomic comparison of serum samples of heat-stressed and

455   normal-temperature buffalo. (a) Principal components analysis (PCA). (b) Volcano plot

456   representation of moderated t-test analysis. Each point represents one protein. Fold

457   change calculated based on the average of six samples. The horizontal bar represents a

458   q-value cutoff of 0.01. Significantly more abundant proteins in the heat-stress buffalo

459   are shown in red; significantly less abundant proteins are shown in green. The

460   significantly more abundant proteins were verified with parallel reaction monitoring

461   analysis.

462   **Figure 2.** Hierarchical clustering of the proteins identified as differentially abundant in

463   the heat-stressed buffalo as compared to the normal-temperature buffalo with label-free

464   quantification analysis. Proteins are in rows; protein details are given in Table 1. Colors

465   indicate level of abundance. HS1–HS6: heat-stress buffalo 1–6; TN1–6: normal-

466   temperature buffalo 1–6. Asterisks indicate proteins that are significantly differently

467   abundant between groups: *$p < 0.05$, **$p < 0.01$.

468   **Figure 3.** Parallel reaction monitoring verification of five of the proteins indicated to

469   be significantly differentially abundant by label-free quantification. HS: heat-stressed

470   buffalo; TN: normal-temperature buffalo. Bars represent means ($n = 6$) ± standard error.

471   Asterisks indicate significant differences in abundance between the two groups: *$p <$

472   0.05, **$p < 0.01$. L8I5R0 and D2U6Z5 represent CP. For full protein names, please

473   refer to Table 1.

474   **Figure 4.** Protein–protein interaction network including the proteins differentially

475   abundant in heat-stressed buffalo as compared to normal-temperature buffalo. Blue

476   edges indicate co-occurrence evidence; purple edges indicate experimental evidence;

477   yellow edges indicate text-mining evidence; light blue edges indicate database evidence;

478   and black edges indicate co-expression evidence. For full protein names, please refer

479   to Table 1.

480   **Figure 5.** Blood parameters of heat-stressed (black bars) and normal-temperature (gray

481   bars) buffalo. WBC: white blood cells ($\times 10^9$); RBC: red blood cells ($\times 10^{12}$); MCHC:

482   mean corpuscular hemoglobin concentration (g/L); MCV: mean corpuscular volume

483   (fL); Hb: hemoglobin (g/L); MCH: mean corpuscular volume (pg); PLT: platelet

484   hematocrit ($\times 10^9$). Bars represent means (n = 6) $\pm$ standard error. Asterisks indicate

485   significant differences in abundance between the two groups: *$p < 0.05$, ***$p < 0.001$.

486   **Figure 6.** A proposed model of heat stress adaptation in dairy buffalo. Proteins and

487   metabolites in red or blue are significantly more or less abundant in heat-stressed

488   buffalo as compared to normal-temperature buffalo.

489

490   **References**

1. http://www.fao.org/faostat/en/#data/QA

2. Intergovernmental Panel on Climate Change in Climate Change: The Science of Climate Change, eds. Houghton, J. T.; Meira Filho, L. G.; Bruce, J.; Lee, H.; Callender, B. A.; Haites, E.; Harris, N.; Maskell, K. (Cambridge Univ. Press, Cambridge, U.K.) 1995.

3. Marai, I. F. M.; Haeeb, A. A. M. Buffalo's biological functions as affected by heat stress — A review. Livest Science. **2010**, *127,* 89-109.

4. Raval, J. K.; Patel, K. M.; Patel, J. M.; Mehta, H. D. Effect of climate on reproductive parameters of surati buffaloes reared under surati buffalo calf rearing project, Gujarat, Research in Environment and Life Sciences. **2014**, *7,* 197-200.

5. Chiappini, U.; Christiaens, J. P. A. Cooling in animal houses. 2nd report of working group on climatization of animal houses. CIGR, State University of Gent. Belgium. **1992**, 82-97.

6. Zhang, C. X. Chinese Buffalo science, Guangxi Science and Technology Press. **2000**, 11.

7. Wheelock, J. B., Rhoads, R. P.; Vanbaale, M. J.; Sanders, S.R.; Baumgard, L. H. Effects of heat stress on energetic metabolism in lactating holstein cows. J. Dairy. Sci. **2010**, *93,* 644-655.

8. Baumgard, L. H.; Rhoads, R. P. Effects of heat stress on postabsorptive metabolism and energetics. Annu. Rev. Anim. Biosci. **2013**, *1,* 311-337.

9. Aggarwal, A.; Upadhyay, R. C. Studies on evaporative heat loss from skin and pulmonary surfaces in male buffaloes exposed to solar radiations. Buffalo J. **1998**, 2, 179–187.

10. Chanda, T.; Debnath, G. K.; Khan, K. I.; Rahman M. M.; Chanda, G. C. Impact of heat stress on milk yield and composition in early lactation of Holstein Friesian crossbred cattle. Bang. J. Anim. Sci. **2017**, *46,* 192-197.

11. Renaudeau, D.; Collin, A.; Yahav, S.; de Basilio, V.; Gourdine J. L.; Collier, R. J. Adaptation to hot climate and strategies to alleviate heat stress in livestock production. Animal. **2012**, *6,* 707-728.

12. Ganaie, A. H.; Shanker, G.; Bumla, N. A.; Ghasura, R. S.; Mir, N. A.; Wani, S. A.; Dudhatra, G. B. Biochemical and physiological changes during thermal stress in bovines: a review. J. Vet. Sci. Technol. **2013**, *4,* 423–430.

13. Kapila, N.; Kishore, A.; Sodhi, M.; Sharma, A. K.; Mohanty, A. K.; Kumar, P.; Mukesh, M. Temporal changes in mRNA expression of heat shock protein genes in mammary epithelial cells of riverine buffalo in response to heat stress in vitro. International Journal of Animal Biotechnology. **2013**, *3,* 5-9.

14. Dunshea, F. R.; Leury, B. J.; Fahri, F.; Digiacomo, K.; Hung, A.; Chauhan, S.; Clarke, I. J.; Collier, R.; Little, S.; Baumgard, L.; Gaughan, J. B. Amelioration of thermal stress impacts in dairy cows. Anim. Prod. Sci. **2013**, *53,* 965-975.

15. Lord-Fontaine, S.; Averill-Bates, D. A. Heat shock inactivity cellular antioxidant defenses against hydrogen peroxide: protection by glucose. Free. Radic. Biol. Med. **2002**, *32,* 752–765.

16. Glombowsky, P.; Bottari, N. B.; Klauck, V.; Fávero, J. F.; Soldá, N. M.; Baldissera, M. D.; Perin, G.; Morsch, V. M.; Schetinger, M. R. C.; Stefani, L. M.; Da Silva, A.

S.   Oxidative stress in dairy cows seropositives for neospora caninum. Comp. Immunol. Microb. **2017**, *54,* 34.

17. Ghosh, C. P.; Kesh, S. S.; Tudu, N. K.; Datta, S. Heat Stress in Dairy Animals - Its Impact and Remedies: A Review. Int. J. App. Pure. Biosci. **2017**, *5,* 953-965.

18. Slimen, B.; Najar, T.; Ghram, A.; Abdrrabba, M. Heat stress effects on livestock: molecular, cellular and metabolic aspects, a review. J. Anim. Physiol. An. A. **2016**, 100, 401–412.

19. Hozyen, H. F.; Ahmed, H. H.; Essawy, G. E. S.; Shalaby, S. I. A. Seasonal changes in some oxidant and antioxidant parameters during folliculogenesis in Egyptian buffalo. Anim. Reprod. Sci. **2014**, *151*, 131-136.

20. Megahed, G. A.; Anwar, M. M.; Wasfy, S. I.; Hammadeh, M. E. Influence of heat stress on the cortisol and oxidant-antioxidants balance during oestrous phase in buffalo-cows (Bubalus bubalis): thermo-protective role of antioxidant treatment. Reprod. Domest. Anim. **2008**, *43,* 672-677.

21. Paula, F. F. Heat stress induced alteration in bovine oocytes: functional and cellular aspects. Anim. Reprod. **2012**, *9,* 395-403.

22. Sordillo, L. M. Selenium-dependent regulation of oxidative stress and immunity in periparturient dairy cattle. Veterinary Medicine International. **2013**, http://dx.doi.org/10.1155/2013/154045

23. Bassols, A.; Turk, R.; Roncada, P. A proteomics perspective: from animal welfare to food safety. Curr. Protein. Pept. Sc. **2014**, *15,* 156-168.

24. Neilson, K. A.; Ali, N. A.; Muralidharan, S.; Mirzaei, M.; Mariani, M.; Assadourian,

G.; Lee, A.; van Sluyter, S. C.; Haynes, P. A. Less label, more free: Approaches in label-free quantitative mass spectrometry. Proteomics. **2011**, *11, 535–553.*

25. Nahnsen, S.; Bielow, C.; Reinert, K.; Kohlbacher, O. Tools for label-free peptide quantification. Mol. Cell. Proteomics. **2013**, *12, 549-556.*

26. Peterson, A. C.; Russell, J. D.; Bailey, D. J.; Westphall, M. S. Parallel reaction monitoring for high resolution and high mass accuracy quantitative, targeted proteomics. Mol. Cell. Proteomics. **2012**, *11, 1475–1488.*

27. Sweredoski, M. J.; Moradian, A.; Raedle, M.; Franco, C.; Hess, S. High resolution parallel reaction monitoring with electron transfer dissociation for middle-down proteomics. Anal. Chem. **2015**, *87, 8360-8366.*

28. Liu, L.; Wang, A.; Chen, J. Blood-based amyloid and tau biomarker tests for alzheimerâs disease. Neuroscience & Biomedical Engineering. **2016**, *4.*

29. Gu, Z. B.; Li, L.; Tang, S. Q.; Liu, C. B.; Fu, X. H.; Shi, Z. X.; Mao, H. M. Metabolomics reveals that crossbred dairy buffaloes are more thermotolerant than Holstein cows under chronic heat stress. J. Agr. Food. Chem. **2018**, DOI: 10.1021/acs.jafc.8b02862

30. Kim, W. S.; Lee, J. S.; Jeon, S. W.; Peng, D. Q.; Kim, Y. S.; Bae, M. H.; Jo, Y. H.; Lee, H. G. Correlation between blood, physiological and behavioral parameters in beef calves under heat stress. Asian. Austral. J. Anim Sci. **2018**, *31, 919-925.*

31. https://www.uniprot.org/uniprot/P69905

32. Zerounian, N. R.; Linder, M. C. Effects of copper and ceruloplasmin on iron

transport in the caco 2 cell intestinal model. J. Nutr. Biochem. **2002**, *13,* 138-148.

33. Chang, Y. Z.; Qian, Z. M.; Du, J. R.; Zhu, L.; Xu, Y.; Li, L.Z.; Wang, C.Y.; Wang, Q.; Ge, X.H.; Ho, K.P.; Niu, L.; Ke, Y. Ceruloplasmin expression and its role in iron transport in c6 cells. Neurochem. Int. **2017**, *50*, 726-733.

34. Pisoschi, A.M.; Pop, A. The role of antioxidants in the chemistry of oxidative stress: a review. Eur. J. Med. Chem. **2015**, *97,* 55–74.

35. Rhoads, M. L.; Rhoads, R. P.; VanBaale, M. J.; Collier, R. J.; Sanders, S. R.; Weber, W. J.; Crooker, B. A.; Baumgard, L. H. Effects of heat stress and plane of nutrition on lactating Holstein cows: I. Production, metabolism, and aspects of circulating somatotropin. J. Dairy. Sci. **2009**, *92,* 1986–1997.

36. Bobek, S.; Sechman, A.; Wieczorek, E.; Wronska-Fortuna, D.; Koziec, K.; Niezgoda, J. Responses of heat stressed chickens to exogenous reverse triiodothyronine (rT3). Transboundary & Emerging Diseases. **1996**, *43,* 521.

37. Koch, F.; Lamp, O.; Eslamizad, M.; Weitzel, J.; Kuhla, B. Metabolic response to heat stress in late-pregnant and early lactation dairy cows: implications to liver-muscle crosstalk. Plos. One. **2016**, *11,* e0160912.

38. Yang, L. The function of hydrogen peroxide as signal molecules-the feedback regulation of hydrogen peroxide on respiratory burst in human np. Science Technology & Engineering. 2002.

39. Adachi, M.; Liu, Y. H.; Fujii, K.; Calderwood, S. K.; Nakai, A.; Imai, K.; Shinomura, Y. Oxidative stress impairs the heat stress response and delays unfolded protein

recovery, Plos. One. **2009**, *4,* e7719.

40. Kho, C. W.; Lee, P. Y.; Bae, K. H.; Kang, S.; Cho, S.; Lee, D. H.; Sun, C. H.; Yi, G. S.; Park, B. C.; Park, S. G. Gpx3-dependent responses against oxidative stress in Saccharomyces cerevisiae. J. Microbiol. Biotechnol. **2018**, *18,* 270-82.

41. Brigelius-Flohe, R. Tissue-specific functions of individual glutathione peroxidases. Free. Radic. Biol. Med. **1999**, *27,* 951-965.

42. Pan, L.; Bu, D. P.; Wang, J. Q.; Cheng, J. B.; Sun, X. Z.; Zhou, L. Y.; Qin, J. J.; Zhang, X. K.; Yuan, Y. M. Effects of Radix Bupleuri extract supplementation on lactation performance and rumen fermentation in heat-stressed lactating Holstein cows. Anim. Feed. Sci. Tech. **2014**, *187,* 1–8.

43. Akbarian, A.; Golian, A.; Kermanshahi, H.; De, S. S.; Michiels, J. Antioxidant enzyme activities, plasma hormone levels and serum metabolites of finishing broiler chickens reared under high ambient temperature and fed lemon and orange peel extracts and curcuma xanthorrhiza essential oil. J. Anim. Physiol. An. N. **2015**, *99,* 150-162.

44. Hu, Y.; Cai, M. C.; Wang, L.; Lin, T.; Wu, B.; Zhang, J. H.; Zuo, F. Y. The serum biochemical indexes and miRNA expression in cattle under heat stress and their correlation analysis. Acta Veterinaria at Zootechnica Sinica. **2016**, *47,* 1840-1847.

45. Cheng, J. B.; Fan, C.Y.; Sun, X. Z.; Wang, J. Q.; Zheng, N.; Zhang, X. K.; Qin, J. J.; Wang, X. M. Effects of bupleurum, extract on blood metabolism, antioxidant status and immune function in heat-stressed dairy cows. J. Integr. Agr. **2018**, *17,* 657-663.

46. Guo, J.; Gao, S.; Quan, S.; Zhang, Y.; Bu, D.; Wang, J. Blood amino acids profile responding to heat stress in dairy cows. Asian. Austral. J. Anim. Sci. **2018**, *31,* 47-53.

47. Zhang, J. X.; Wang, R.; Xi, J.; Shen, L.; Zhu, A. Y.; Qi, Q.; Wang, Q. Y.; Zhang, L. J., Wang, F. C.; Lü, H. Z.; Hu, J. G. Morroniside protects SK-N-SH human neuroblastoma cells against H_2O_2-induced damage. Int. J. Mol. Med. **2017**, *39,* 603-612.

48. Zhang, F. J.; Weng, X. G.; Wang, J. F.; Zhou, D.; Zhang, W.; Zhai, C. C.; Hou, Y. X.; Zhu, Y. H. Effects of temperature-humidity index and chromium supplementation on antioxidant capacity, heat shock protein 72, and cytokine responses of lactating cows. J. Anim. Sci. **2014**, *92,* 3026-3034.

49. Tomasinsig, L.; De Conti, G.; Skerlavaj, B.; Piccinini, R.; Mazzilli, M.; D'Este, F.; Tossi, A.; Zanetti, M. Broad-spectrum activity against bacterial mastitis pathogens and activation of mammary epithelial cells support a protective role of neutrophil cathelicidins in bovine mastitis. Infect. Immun. **2010**, *78,* 1781-1788.

50. Whelehan, C. J.; Barry-Reidy, A.; Meade, K. G.; Eckersall, P. D.; Chapwanya, A.; Narciandi, F.; Lloyd, A. T.; O'Farrelly, C. Characterisation and expression profile of the bovine cathelicidin gene repertoire in mammary tissue. BMC Genomics. **2014**, *15,* 128-128.

51. Kozłowska, E.; Wysokiński, A.; Brzezińska-Błaszczyk, E. Serum levels of peptide cathelicidin ll-37 in elderly patients with depression. Psychiat. Res. **2017**, *255,* 156-160.

52. Young-Speirs, M.; Drouin, D.; Cavalcante, P.   A.; Barkema, H. W.; Cobo, E. R.

Host defense cathelicidins in cattle: types, production, bioactive functions and potential therapeutic and diagnostic applications. Int. J. Antimicrob. Ag. **2018**, *51,* 813-821.

53. Radek, K. A.; Elias, P. M.; Taupenot, L.; Mahata, S. K.; O'Connor, D. T.; Gallo, R. L. Neuroendocrine nicotinic receptor activation increases susceptibility to bacterial infections by suppressing antimicrobial peptide production. Cell. Host. Microbe. **2010**, *7,* 277-289.

54. Sheeba, V.; Arunachalam, P.; Swarnalatha, K. Correlation of hemoglobin with creatinine clearance, antioxidant status, lipid peroxidation and ceruloplasmin in patients with chronic kidney disease. Inter. J. Res. Med. Sci. **2016**, 4, 4487-4492.

55. Young-Speirs, M.; Drouin, D.; Cavalcante, P. A.; Barkema, H. W.; Cobo, E. R. Host defense cathelicidins in cattle: types, production, bioactive functions and potential therapeutic and diagnostic applications. Int. J. Antimicrob. Ag. **2018**, *51,* 813-821.

56. McNamara, T. C.; Keen, J. T.; Simmons, G. H.; Alexander, L. M.; Wong, B. J. Endothelial nitric oxide synthase mediates the nitric oxide component of reflex cutaneous vasodilatation during dynamic exercise in humans. J. Physiol. **2014**, *592,* 5317–5326

57. Koga, A.; Ishikawa, N.; Tajima, A.; Homma, H.; Kanai, Y.; Chikamune, T. Characteristics of Physiological Responses and Blood Constituents in Relation to Seasonal Changes of the Environment in Buffaloes Compared with Cattle. Japan. J. Trop. Agr. **1991**, *35,* 283-288.

58. Gomeza, J.; Shannon, H.; Kostenis, E.; Felder, C.; Zhang, L.; Brodkin, J.; Grinbeng,

A.; Sheng, H.; Wess, J. Pronounced pharmacologic deficits in m2 muscarinic acetylcholine receptor knockout mice. Proceedings of the National Academy of Sciences of the United States of America. **1999**, *96,* 1692-1697.

59. Kumar, S. Glutamic acid as a precursor of acetylcholine synthesis in rat brain in vivo. Observations on the compartmentalization. Brain Research. **1971**, *33*, 578-580.

60. Main, P. A.; Angley, M. T.; O'Doherty, C. E.; Thomas, P.; Fenech, M. The potential role of the antioxidant and detoxification properties of glutathione in autism spectrum disorders: a systematic review and meta-analysis. Nutr. Metab. **2012**, *9,* 35.

61. Xu, X.; Leng, J. Y.; Gao, F.; Zhao, Z. A.; Deng, W. B.; Liang, X. H.; Zhang, Y. J.; Zhang, Z. R.; Li, M.; Sha, A. G.; Yang, Z. M. Differential expression and anti-oxidant function of glutathione peroxidase 3 in mouse uterus during decidualization. FEBS Letters. **2014**, *588,* 1580-1589.

62. Wilson, N. E.; Stricker, E. M. Thermal homeostasis in pregnant rats during heat stress. Journal of Comparative and Physiological Psychology. **1979**, *93,* 585-594.

63. Horowitz, M.; Meiri, U. Altered responsiveness to parasympathetic activation of submaxillary salivary gland in the heat-acclimated rat. Comp. Biochem. Physiol. A. Comp. Physiol. **1985**, *80,* 57–60

64. GonzálezAlonso, J.; Calbet, J. A. Reductions in systemic and skeletal muscle blood flow and oxygen delivery limit maximal aerobic capacity in humans. Circulation.

2003, *107,* 824-830.

65. Pizzuti, C.; Rombo, S. E. Algorithms and tools for protein–protein interaction networks clustering, with a special focus on population-based stochastic methods. Bioinformatics. **2014**, *30,* 1343-1352.

66. Osaki, S.; Johnson, D. A.; Frieden, E. The possible significance of the ferrous oxidase activity of ceruloplasmin in normal human serum. J. Bio. Chem. **1966**, *241,* 2746-2751.

67. Fosset, C.; McGaw, B. A.; Abramovich, D.; Mcardle, H. J. Interrelations between ceruloplasmin and Fe status during human pregnancy. Biol. Trace. Elem. Res. **2004**, *98,* 1.

68. Tetik, V.A.; Harman, E.; Bozok, Ç. V.; Kayıkçıoğlu, M.; Vardarl, E.; Zengi, A.; Şahin, A. K.; Eroğlu, Z. Polymorphisms of lipid metabolism enzyme-coding genes in patients with diabetic dyslipidemia. Anatol. J. Cardiol. **2017**, 17, 313-321.

69. Cemek, M.; Caksen, H.; Bayiroğlu, F.; Cemek, F.; Dede, S. Oxidative stress and enzymic–non-enzymic antioxidant responses in children with acute pneumonia. Cell Biochemistry & Function. **2010**, *24,* 269-273.

70. Sreedhar, R.; Arumugam, S.; Thandavarayan, R. A.; Giridharan, V. V.; Karuppagounder, V.; Pitchaimani, V.; Afrin, R.; Miyashita, S.; Nomoto, M.; Harima, M.; Gurusamy, N.; Suzuki, K.; Watanabe, K. Myocardial 14-3-3η protein protects against mitochondria mediated apoptosis. Cell. Signal. **2015**, *27,* 770-776.

71. Collin, A.; Lebreton, Y.; Fillaut, M.; Vincent, A.; Thomas, F.; Herpin, P. Effects of exposure to high temperature and feeding level on regional blood flow and

oxidative capacity of tissues in piglets. Exp. Physiol. **2010**, *86,* 83-91.

72. Bain, A. R.; Morrison, S. A.; Ainslie, P. N. Cerebral oxygenation and hyperthermia. Front. Physiol. **2014**, *5,* 92. doi: 10.3389/fphys.2014.00092.

73. Rubsamen, K.; Hales, J. R. S. Circulatory adjustment of heat-stressed livestock, in Stress physiology in livestock. Basic principles, 1, edited by M.K. Yousef. Boca Raton, Florida: CRC. Press. **1985**, 143-154.

74. Ogoh, S.; Sato, K.; Okazaki, K.; Miyamoto, T.; Hirasawa, A.; Morimoto, K.; Shibasaki, M. Blood flow distribution during heat stress: cerebral and systemic blood flow. J. Cerebr. Blood. F. Met. **2013**, *33,* 1915-1920.

75. Pearce, S. C.; Mani, V.; Boddicker, R. L.; Johnson, J. S.; Weber, T. E.; Ross, J. W.; Rhoads, R. P.; Baumgard, L. H.; Gabler, N. K. Heat stress reduces intestinal barrier integrity and favors intestinal glucose transport in growing pigs. Plos One. **2013**, *8,* e70215.

76. Takahashi, M. Heat stress on reproductive function and fertility in mammals. Reprod. Med. Biol. **2012**, *11,* 37-47

77. Lublin, A.; Wolfenson, D. Lactation and pregnancy effects on blood flow to mammary and reproductive systems in heat stressed rabbits. Comp. Biochem. Physiol. A. Physiol. **1996**, *115,* 277-285.

78. Elseddig, H. The effect of open poultry houses design on physiological performance of layer hens. (2010). University of Khartoum, Master degree.

79. Habeeb, A. A. M. The role of insulin in improving productivity of heat stressed farm

animals with different techniques, Zagazig, Egypt: Ph.D. Thesis, Faculty of Agriculture, Zagazig University (1987).

80. Transport of oxygen and carbon dioxide in blood and tissue fluids. In: A.C. Guyton, J.E. Hall. Textbook of Medical Physiology. 11th ed. Philadelphia: Elsevier. **2006**, 503-513.

81. Srikandakumar, A.; Johnson, E.H.; Mahgoub, O. Effect of heat stress on respiratory rate, rectal temperature and blood chemistry in omani and australian merino sheep. Small. Ruminant. Res. **2013**, *49*, 193-198.

82. Mohanty, J. G.; Nagababu, E.; Rifkind, J. M. Red blood cell oxidative stress impairs oxygen delivery and induces red blood cell aging. Front. Physiol. **2014**, *5,* 84.

83. Alam, M. M.; Hashem, M. A.; Rahman, M. M.; Hossain, M. M.; Haque, M. R.; Sobhan, Z.; Islam, M.S. Effect of heat stress on behavior, physiological and blood parameters of goat. Progressive. Agriculture. **2013**, *22,* 37-45.

84. Rana, M. S.; Hashem, M. A.; Sakib, M. N.; Kumar, A. Effect of heat stress on blood parameters in indigenous sheep. Journal of the Bangladesh Agricultural University. **2014**, *12,* 91-94.

85. Waltz, X.; Baillot, M.; Connes, P.; Bocage, B.; Renaudeau, D. Effects of hydration level and heat stress on thermoregulatory responses, hematological and blood rheological properties in growing pigs. Plos One. **2014**, *9*, e102537-e102537.

86. Qiang, J.; Bao, W. J.; Tao, F. Y.; He, J.; Li, X. H.; Xu, P.; Sun, L. Y. The expression profiles of mirna–mrna of early response in genetically improved farmed tilapia

(oreochromis niloticus) liver by acute heat stress. Sci. Rep. **2017**, *7*. DOI:10.1038/s41598-017-09264-4

87. Srikandakumar, A.; Johnson, E.H. Effect of heat stress on milk production, rectal temperature, respiratory rate and blood chemistry in Holstein, Jersey and Australian Milking Zebu cows. Trop. Animal. Health. Prod. **2004**, *36,* 685-692.

88. Silva, R.G.; da Costa M.J.; Sobrinho, A.G. Influence of hot environments on some blood variables of sheep. Int. J. Biometeorol. **1992**, *36,* 223-225.

89. Tucker, C. B.; Rogers, A. R.; Schütz, K. E. Effect of solar radiation on dairy cattlebehaviour: use of shade and body temperature in a pasture-based system. Appl. Anim. Behav. Sci. **2008**, 109, 141–154.

90. Brijesh, Y.; Vijay, P.; Sarvajeet, Y.; Yajuvendra, S.; Vinod, K.; Rajneesh, S. Effect of misting and wallowing cooling systems on milk yield, blood and physiological variables during heat stress in lactating murrah buffalo. J. Anim. Sci. Technol. **2018**, *58,* 2. DOI: 10.1186/s40781-015-0082-0

91. Sivakumar, A. V. N.; Singh, G.; Varshney, V. P. Antioxidants supplementation on acid base balance during heat stress in goats. Asian. Austral. J. Anim. Sci. **2000**, *23*, 1462-1468.

92. Xin, W. U.; Li, Z. Y.; Jia, A. F.; Su, H.G.; Hu, C.H.; Zhang, M.H.; Feng, J.H. Effects of high ambient temperature on lipid metabolism in finishing pigs. J. Integr. Agr. **2016**, *15,* 391-396.

93. Ricartjané, D.; Cejudomartín, P.; Peinadoonsurbe, J.; Lópeztejero, M. D.; Llobera,

M. Changes in lipoprotein lipase modulate tissue energy supply during stress. J. Appl. Physiol. **2005**, *99,* 1343-1351.

94 Sturm, R.; Sheynkman, G.; Booth, C.; Smith, L. M.; Pedersen, J. A.; Li, L. Absolute quantification of prion protein (90-231) using stable isotope-labeled chymotryptic peptide standards in a LC-MRM AQUA workflow. J. Am. Soc. Mass Spectrom. **2012**, 23, 1522-1533.

95. Larsen, T. S.; Lagercrantz, H.; Riemersma, R. A.; Blix, A. S. Seasonal changes in blood lipids, adrenaline, noradrenaline, glucose and insulin in norwegian reindeer. Acta. Physiol. **1984**, *124,* 53-59.

96) Kouba, M.; Hermier, D.; Dividich, J. L. Influence of a high ambient temperature on lipid metabolism in the growing pig. J. Anim. Sci. **2001**, *79,* 81–87.

97 . Qu, H.; Donkin, S. S.; Ajuwon, K. M. Heat stress enhances adipogenic differentiation of subcutaneous fat depot-derived porcine stromovascular cells. J. Anim. Sci. **2015**, *93,* 3832-3842.

98) Mayer, M. L.; Hancock, R. E. Cathelicidins link the endocrine and immune systems. Cell. Host. Microbe. **2010**, *7,* 257-259.

99. Fuquay, J. W.; Zook, A. B.; Daniel, J. W.; Brown, W. H.; Poe, W. E. Modifications in free stall housing for dairy cows during summer. J. Dairy. Sci. **1979**, *62,* 566-577.

100. West, J. W. Effects of heat-stress on production in dairy cattle: a review. J. Dairy. Sci. **2003**, *86,* 2131-2144.

101 . Wisniewski, J. R.; Zougman, A.; Nagaraj, N.; Mann, M. Universal sample preparation method for proteome analysis. Nat. Methods. **2009**, *6,* 359-362.

102 . Cox, J.; Mann, M. MaxQuant enables high peptide identification rates, individualized p.p.b.-range mass accuracies and proteome-wide protein quantification. Nat. Biotechnol. **2008**, *26,* 1367-1372.

103. Cox, J.; Neuhauser, N.; Michalski, A.; Scheltema, R. A.; Olsen, J. V.; Mann, M. Andromeda: a peptide search engine integrated into the maxquant environment. J. Proteome. Res. **2011**, *10,* 1794-1805.

104. Cox, J.; Hein, M. Y.; Luber, C. A.; Paron, I.; Nagaraj, N.; Mann, M. Accurate proteome-wide label-free quantification by delayed normalization and maximal peptide ratio extraction, termed maxlfq. Mol. Cell. Proteomics. **2014**, *13,* 2513-2526.

105 . Saldanha, A. J. Java Treeview–extensible visualization of microarray data. Bioinformatics. **2004**, *20,* 3246-3248.

106 . MacLean, B.; Tomazela, D. M.; Shulman, N.; Chambers, M.; Finney, G. L.; Frewen, B.; Kern, R.; Tabb, D. L.; Liebler, D. C.; MacCoss, M. J. Skyline: an open source document editor for creating and analyzing targeted proteomics experiments. Bioinformatics. **2010**, *26,* 966-968.

107. Lin, M. M.; Fang, J. B.; Qi, X. J.; Li, Y. K.; Chen, J. Y.; Sun, L. M.; Zhong, Y. P. iTRAQ-based quantitative proteomic analysis reveals alterations in the metabolism of actinidia arguta. Sci. Rep. **2017**, *7.*

108. Quevillon, E.; Silventoinen, V.; Pillai, S.; Harte, N.; Mulder, N.; Apweiler, R.; Lopez, R. Interproscan: protein domains identifier. Nucleic. Acids. Res. **2005**, *33,* 116-120.

109. Ashburner, M.; Ball, C. A.; Blake, J. A.; Botstein, D.; Butler, H.; Cherry, J. M.; Davis, A. P .; Dolinski, K.; Dwight, S. S.; Eppig, J. T.; Harris, M. A.; Hill, D. P.; Issel-Tarver, L.; Kasarskis, A.; Lewis, S.; Matese, J. C.; Richardson, J. E.; Ringwald, M.; Rubin, G. M.; Sherlock, G. Gene ontology: tool for the unification of biology. The Gene Ontology Consortium. Nat. Genet. **2000**, *25,* 25-29.

110. Götz, S.; Garcíagómez, J. M.; Terol, J.; Williams, T. D.; Nagaraj, S. H.; Nueda, M. J.; Robles, M.; Talón, M.; Dopazo, J.; Conesa, A. High-throughput functional annotation and data mining with the blast2go suite. Nucleic. Acids. Res. **2008**, *36,* 3420-3435.

111. Kanehisa, M.; Goto, S.; Sato, Y.; Furumichi, M.; Tanabe, M. KEGG for integration and interpretation of large-scale molecular data sets. Nucleic. Acids. Res. **2012**, *40,* 109-114.

Table 1. Proteins Differentially Abundant in Heat-stressed Buffalo as Compared

to Normal-temperature Buffalo, as Indicated by Label-free Quantitation

Protein ID	Protein symbol	Protein name	Fold change	P
Q9TSN7	HBA1	Hemoglobin subunit alpha1	3.76	0.036
L8I5R0	CP	Ceruloplasmin,	1.50	0.024
A0A0A7V3V9	CAMP (LL-37)	Cathelicidin-2, CATHL2	1.84	0.026
D2U6Z5	CP	Ceruloplasmin	1.58	0.035
P63103	YWHAZ	YWHAZ	0.35	0.001
P37141	GPX3	Glutathione peroxidase 3	0.35	0.006
K9MNT8	RETN	Resistin	0.47	0.022
Q2KII3	HAVCR1	Hepatitis A virus cellular receptor 1 N-terminal domain containing protein	0.44	0.030
P62261	YWHAE	Protein epsilon	0.52	0.001
G5E5V0	CPN1	Carboxypeptidase N catalytic chain precursor	0.63	0.007
E1ACW2	LPL	Lipoprotein lipase	0.59	0.010
A7Z057	YWHAG	Protein gamma	0.51	0.017
L8I9P7	CD14	Monocyte differentiation antigen	0.65	0.020
L8I6N0	CHST4	Glycosylation-dependent cell adhesion molecule 1,	0.59	0.022
L8IDW3	THBS4	Thrombospondin-4	0.57	0.033
L8IZ21	SERPINF1	Pigment epithelium-derived factor	0.65	0.034
L8HYL8	PLA1A	Phospholipase A1 member A	0.56	0.045

Table 2. Gene Ontology (GO) Analysis of the Proteins Differentially Abundant in Heat-stressed Buffalo as Compared to Normal-temperature Buffalo

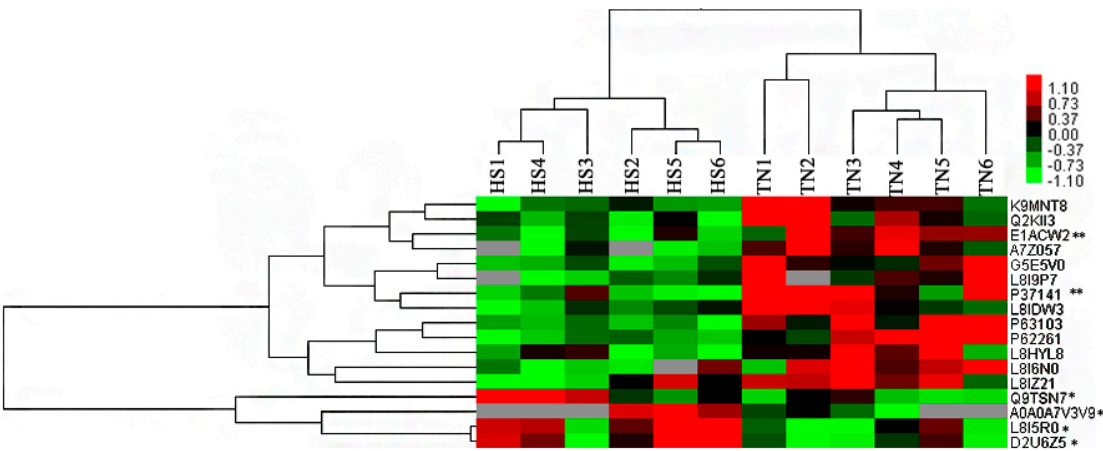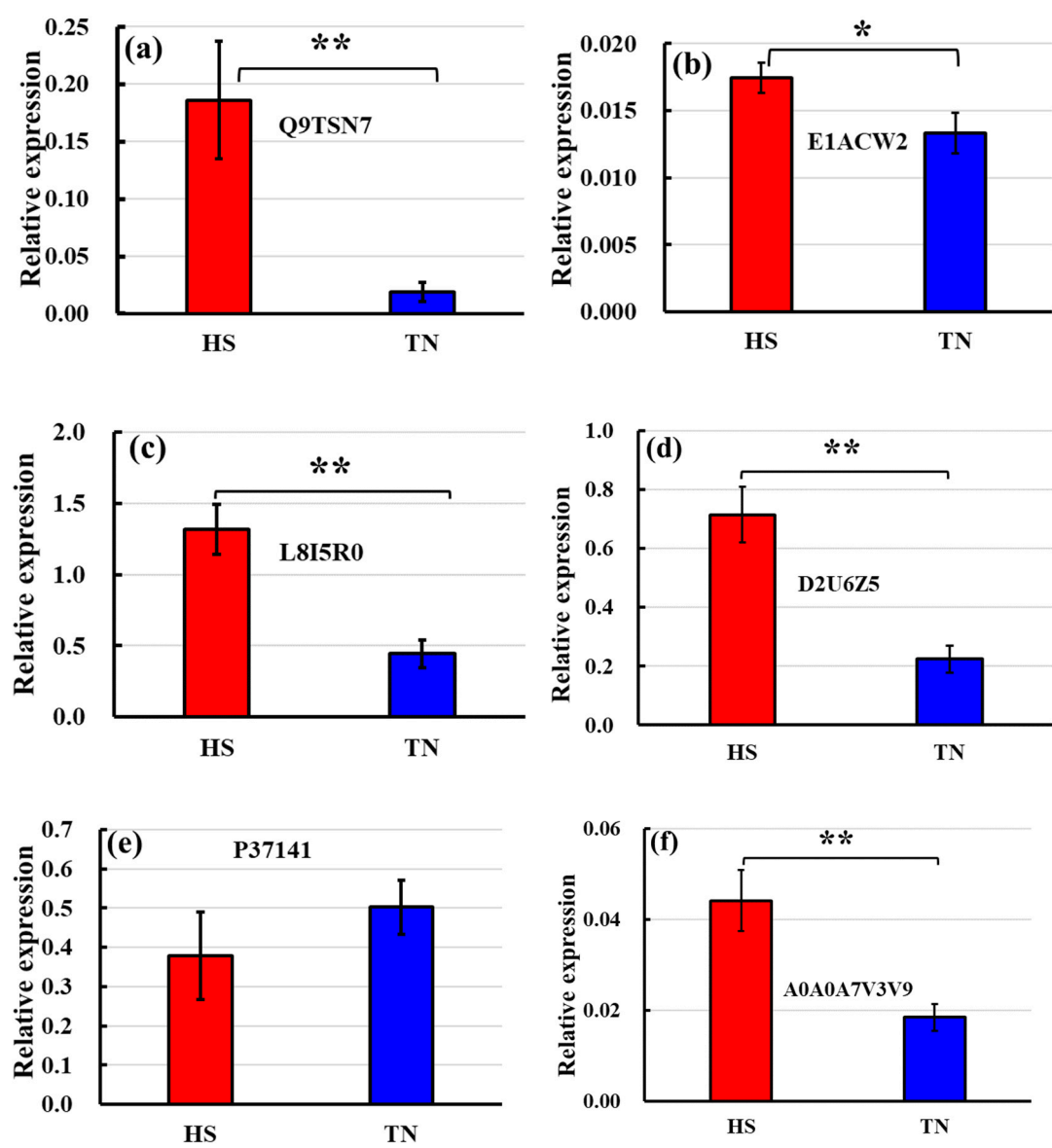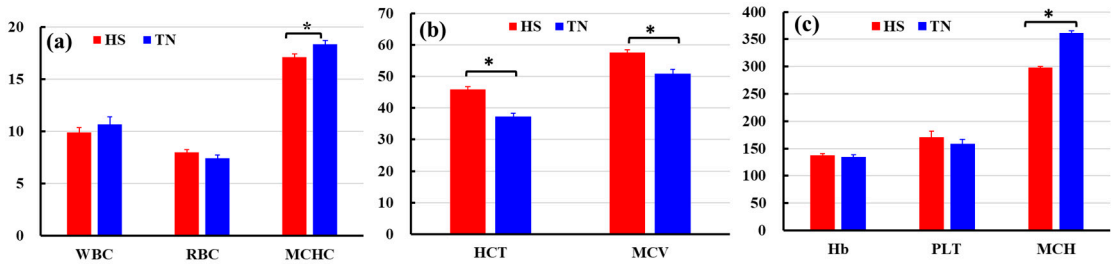| GO_ID	GO term	Proteins associated
GO:0004602	Glutathione peroxidase activity	P37141
GO:0016787	Hydrolase activity	E1ACW2, G5E5V0, L8HYL8
GO:0019825	Oxygen binding	Q9TSN7
GO:0016491	Oxidoreductase activity	L8I5R0, P63103, P62261, A7Z057, P37141, D2U6Z5
GO:0030235	Nitric-oxide synthase regulator activity	L8IAK0
GO:0051082	Unfolded protein binding	L8IAK0
GO:0031072	Heat shock protein binding	L8IAK0
GO:0004497	Monooxygenase activity	P63103, P62261, A7Z057
GO:0005179	Hormone activity	K9MNT8
GO:0016616	Oxidoreductase activity	L8I5R0
GO:0016298	Lipase activity	E1ACW2, L8HYL8
GO:0004322	Ferroxidase activity	L8I5R0, D2U6Z5
GO:0004806	Triglyceride lipase activity	E1ACW2
GO:0031625	Ubiquitin protein ligase binding	P63103, P62261
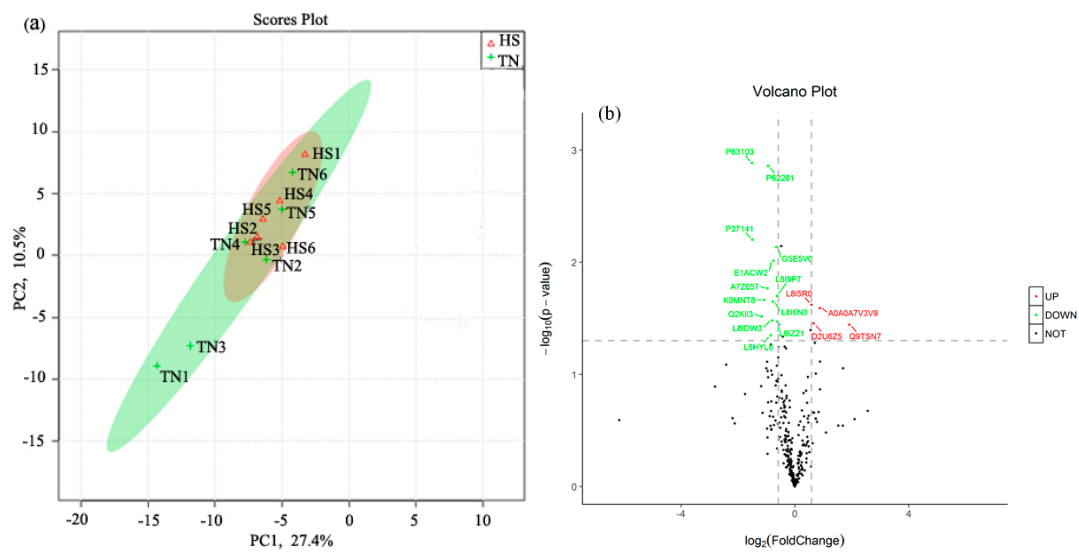
Figure 1.

Figure 2.

Figure 3.

Figure 4.

Figure 5.

Figure 6.